JOURNAL OF OPTOELECTRONICS AND ADVANCED MATERIALS Vol. 12, No. 4, April 2010, p. 872 - 875

Electronic phase diagram of $La_{0.54}Sm_{0.11}Ca_{0.35}Cu_xMn_{1-x}O_3$ manganites

N. CORNEI[a], M.-L. CRAUS[b,c*], M. LOZOVAN[c], O. MENTRÉ[d]
[a]*Department of Chemistry, "Al.I.Cuza" University, Iasi, Romania*
[b]*Institute of Research and Development for Technical Physics, Iasi, Romania*
[c]*Joint Institute of Nuclear Research, Dubna, Russia*
[d]*UCCS, Equipe de Chimie du Solide, ENSCL, Lille, France*

The $Alk_{1-x}Re_xMnO_3$ manganites, where Alk = Sr, Ca, Ba and Re = rare earth, are very well known as magnetoresistive materials near room temperature. The substitution of Mn with other transition cations produces a change of Mn-O-Mn interactions, followed by corresponding change in the electronic phase diagram. The samples with nominal composition $La_{0.54}Sm_{0.11}Ca_{0.35}Mn_{1-x}Cu_xO_3$ (LSCMCO) were prepared as bulk by sol-gel method. We have discussed the dependence of the transition from the metal to insulator behavior and the modification of FM/AFM concentrations for doped with Cu $La_{0.54}Sm_{0.11}Ca_{0.35}MnO_3$ (LSCMCO) manganites.

(Received April 7, 2010; accepted April 26, 2010)

Keywords: magnetoresistance, manganites, crystalline/magnetic structure

1. Introduction

Hole-doped perovskite manganese oxides of the type $Ln_{1-x}A_xMnO_3$, where Ln is a trivalent rare earth and A is a divalent alkaline-earth element, were intensively investigated in the last ten years, due to the observed colossal magnetoresistance (CMR) near ferromagnetic-paramagnetic transition temperature. The CMR effect is most prominent for $x \approx 0.3$. Spin structure and electric properties are controlled by Zener double exchange mechanism [1], despite some experimental results, which cannot be explained by means of double exchange theory. The simultaneous presence of Mn^{3+} and Mn^{4+} ions in Mn^{3+}–O– Mn^{4+} bonds in these compounds is responsible for the appearance of the ferromagnetism as well as the phase transition. Substitution of Mn with Cu cations should lead to a change of lattice parameters and of magnetic structure of the samples. We intend to discuss the transport and magnetic properties, in agreement with the chemical composition and crystalline structure of $La_{0.54}Sm_{0.11}Ca_{0.35}Mn_{1-x}Cu_xO_3$ manganites.

2. Experimental

We have obtained a new type of manganites $La_{0.54}Sm_{0.11}Ca_{0.35}Mn_{1-x}Cu_xO_3$ (x=0.03, 0.06 and 0.10) by sol-gel method.

XRD analysis was performed with a Huber diffractometer at room temperature, data being handled by using the Rietveld refinement method. The samples are single phased, orthorhombic, S.G. Pnma (n°62). The atomic positions, lattice parameters and some microstructure parameters were obtained by using Full Prof program. Magnetic measurements were performed with a Foner type magnetometer between 77 and 300 K. The dependence of the resistivity with temperature and the applied magnetic field was determined between 4 and 300 K with a Maglab EXA9T magnetometer.

3. Results and discussion

The sintered samples contain only a phase, which have an orthorhombic structure, Pmna (see Table 1 and Figs. 1 and 2), in agreement with the literature [2, 3]. The cell parameters have been refined through the profile matching stage of the Rietveld refinement [4] (see Table 1 and Fig. 2).

Table 1. Atomic positions and equivalent isotropic displacement parameters (B_{eq}) for $La_{0.54}Sm_{0.11}Ca_{0.35}Mn_{0.9}Cu_{0.1}O_3$ manganites

Atom	site	x	y	z	B_{eq}(Å^2)
La,Sm,Sr	4c	0.0202	0.2500	-0.0084	0.469
Mn,Cu	4b	0.0000	0.0000	0.5000	0.860
O_{ap}	4c	0.4848	0.2500	0.0770	0.151
O_{ap}	8d	0.2065	-0.0210	0.7810	0.151

Note: Equivalent isotropic temperature factors are computed according to the relation $B_{eq} = 4/3\Sigma_{ij}\beta_{ij}a_ia_j$.

Table 2. Lattice constants (a, b, c), volume of the unit cell (V), average size of the mosaic blocks (D) and the microstrains (ε) of LSCMCO manganites.

x	a (Å)	b (Å)	c (Å)	V ($Å^3$)	D (Å)	ε ($x10^3$)
0.03	5.447_9	7.685_5	5.447_8	228.10	810	0. 311
0.06	5.441_7	7.706_5	5.439_2	228.10	834	0. 372
0.10	5.448_1	7.686_0	5.447_1	228.09	850	0. 366

In second stage atoms positions and occupancies have been refined on the basis of data from the literature. A small maximum of unit cell volume with Cu concentration was observed (see Table 1).

Table 3. Dependence of calculated B-O and A-O distance (d_{B-O} and d_{A-O}) and of bandwidth (w) on Cu concentration (x).

x	$<r_B>$ (Å)	$\langle d_{BOB} \rangle$ (Å)	$\langle d_{AO} \rangle$ (Å)	$\langle \angle \theta_{MnOMn} \rangle$ (°)
0.03	0.731	1.9825_{ap} 1.9321_{eq}	2.6403	151.355_{ap} 170.046_{eq}
0.06	0.769	1.9707_{ap} 1.9283_{eq}	2.6273	156.150_{ap} 175.196_{eq}
0.10	0.773	1.9685_{ap} 1.9538_{eq}	2.6230	154.920_{ap} 160.655_{eq}

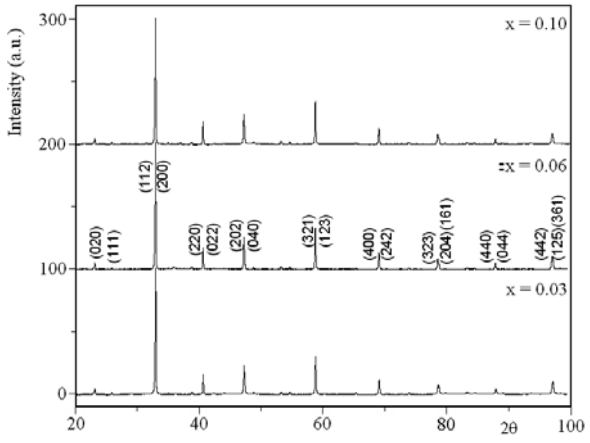

Fig. 1. Diffractograms of LSCMCO manganites.

The average size of A sites should remain constant, while the B site radius should decrease with increase of Cu^{2+} concentration. On other hand, a decrease of oxygen concentration in the manganites could increase the Mn^{3+} concentration, implicitly and the radius of B places, that explains the variation of unit cell volume. Variation of observed or calculated magnetization ($p_{max.\ obs.}$, $p_{max.\ calc.}$) per unit with Cu concentration is monotonous, but the difference between $p_{max.\ obs.}$ and $p_{max.\ calc.}$ decreases with the increase of Cu concentration (see Table 2).

The number of Mn^{3+}-O-Mn^{4+} bonds which participate to the magnetic moment of the samples increase also with the increase of Cu concentration in the samples (see Table 4 and Fig. 3). In the same time, the larger Curie temperature characterizes the LSCMCO with x = 0.10 Cu concentration (s. Table 4).

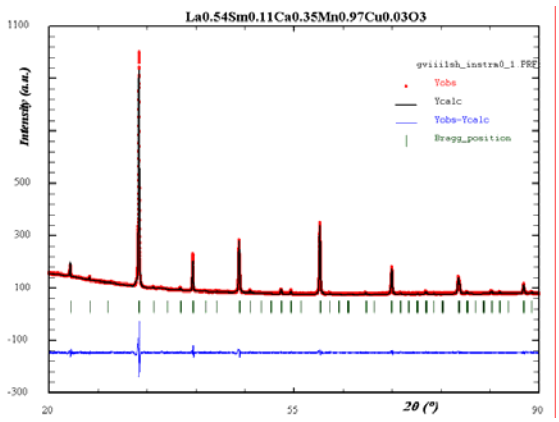

Fig. 2. Observed (red), calculated (black) and difference between observed and calculated diffractograms (magenta). Bragg positions – green vertical bars

Table 4. Variation of Curie temperature (T_C), transition metal-insulator temperatures ($T_{MI,\ intrinsic}$ and $T_{MI,\ extrinsic}$), molar magnetization calculated and observed ($p_{max,\ calc}$ and $p_{max,\ obs}$).

x	T_C (K)	$T_{MI,}$ intrinsic (K)	$T_{MI,}$ extrinsic (K)	$p_{max.\ calc.}$ (μ_B/f.u.)	$p_{max.\ obs.}$ (μ_B/f.u.)
0.03	196.3	196	93	2.584	0.825
0.06	188.4	188	60	2.784	0.993
0.10	199.2	188	106	3.060	2.657

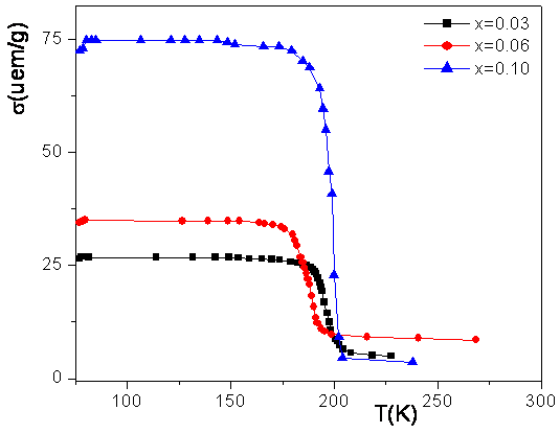

Fig. 3. Variation of specific magnetization with temperature and Cu concentration

We consider that two phases there are in LSCMCO manganites: a ferromagnetic metallic phase and an

antiferromagnetic (paramagnetic) phase. The metallic phase concentration should increase with increase of Cu concentration in the samples, which explains the magnetic behavior of the LSCMCO manganites. Concerning the transport properties, we have obtained a maximum corresponding to extrinsic magnetoresistance (at low temperatures) and maximum corresponding temperatures near Curie temperature, for each sample (see Table 4 and Figs. 4, 5, 6 and 7). Also, a minimum of transition temperature (extrinsic component of magnetoresistance) are correlated with a maximum of microstrains (s. Tables 2 and 4).

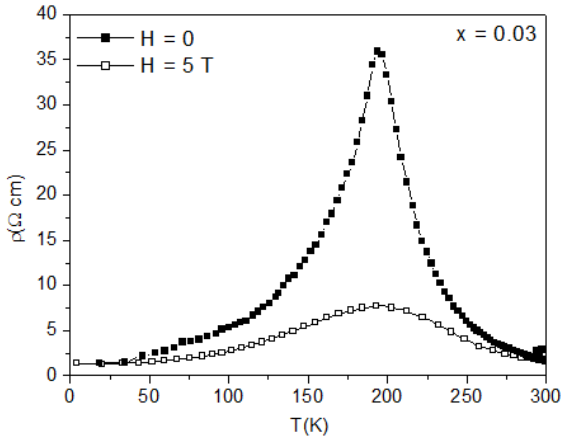

Fig. 4. Variation of resistivity with temperature and intensity of magnetic field for $La_{0.54}Sm_{0.11}Ca_{0.35}Mn_{0.97}Cu_{0.03}O_3$ manganite.

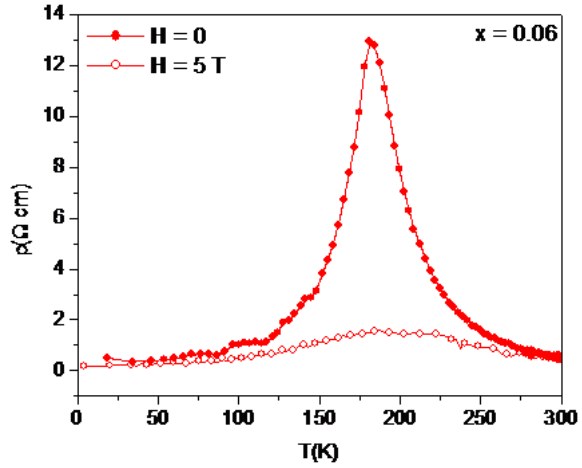

Fig. 5. Variation of resistivity with temperature and intensity of magnetic field for $La_{0.54}Sm_{0.11}Ca_{0.35}Mn_{0.94}Cu_{0.06}O_3$ manganite.

On other hand, it can be observed that the maximum of resistivity with temperature becomes smaller with increase of Cu concentration in the samples (s. Figs. 4, 5 and 6).

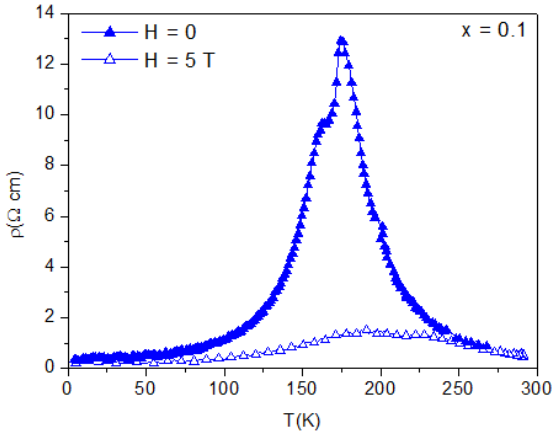

Fig. 6. Variation of resistivity with temperature and intensity of magnetic field for $La_{0.54}Sm_{0.11}Ca_{0.35}Mn_{0.90}Cu_{0.10}O_3$ manganite.

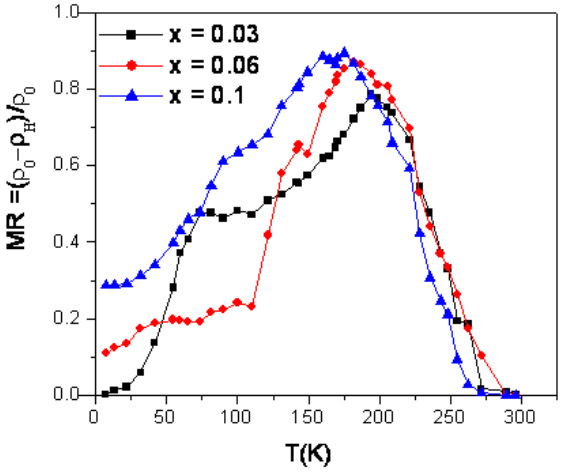

Fig. 4. Variation of magnetoresistance on temperature and Cu concentration.

Despite other data concerning the magnetoresistance, the present data shows a complex behavior with temperature and Cu concentration. Two maxima can be observed: one maximum at high temperature, with was associated with the intrinsic magnetoresistance (see Table 3 and Figure 4), and a second maximum, at lower temperatures, associated with extrinsic magnetoresistance (see Figure 4 and Table 3). The second magnetoresistance maximum is due to the defaults concentration in the crystalline/magnetic lattice, especially in the boundary layers.

Larger maxima, that means a larger distribution of Mn-O distances and Mn-O-Mn angles, around a specific value, are associated with larger defaults concentrations. We attributed the displacement of the second maximum of magnetoresistance to the variation of the Mn-O length and Mn-O-Mn angles, due to the substitution of Mn with Cu and to the variation of O concentration in the samples.

4. Conclusions

We have obtained the $La_{0.54}Sm_{0.11}Ca_{0.35}Mn_{1-x}Cu_xO_3$ manganites bulk by sol-gel method. The LSCMCO manganites crystallize in Pnma space group. The change of Curie temperature and of magnetization per formula unit is associated with the change of Mn-O lengths and Mn-O-Mn angles in the crystalline „core", which have the largest contribution to the magnetic moment of the samples. The increase of Cu cations concentration induces the increase of the symmetry of BO_6 octahedra and polarity of Mn-O bonds. Two transition temperatures were observed: one due to the intrinsic contribution of the crystalline „core" and the second to the extrinsic contribution of the boundary layers. We suppose that the cause of the transition temperature modification is the same in both cases: change of Mn-O lengths and Mn-O-Mn angles. However, in the boundary layers a larger defaults concentration can be found as comparing with those from crystalline „core", that explains the difference between the extrinsic and intrinsic corresponding transition temperatures.

References

[1] C. Zener, Phys. Rev. **82**, 403 (1951).
[2] R. Ran, X. Wu, D. Weng, Journal of Alloys and Compounds **414**, 169 (2006).
[3] N. Balchev, B. Kunev, J. Pirov, A. Souleva, K. Nenkov, Journal of Superconductivity: Incorporating Novel Magnetism **17**, 519 (2004).
[4] J. Rodriguez-Carvajal, T. Roisnel, H. Rietveld – Rietveld Method Web-site, Fullprof (2000).

*Corresponding author: craus@phys-iasi.ro